

Observation of a shape resonance in the collision of two cold ^{87}Rb atoms

H. M. J. M. Boesten,¹ C. C. Tsai,² J. R. Gardner,² D. J. Heinzen,² and B. J. Verhaar¹

¹*Eindhoven University of Technology, Box 513, 5600MB Eindhoven, The Netherlands*

²*University of Texas, Austin, Texas 78712*

(Received 19 July 1996)

We observe a shape resonance in the scattering of two ultracold ^{87}Rb atoms, causing the colliding atoms to form a long-living compound system inside an $l=2$ centrifugal barrier. Its existence follows from a photoassociation experiment in a gas sample of doubly polarized ^{87}Rb atoms. Using it we are able to carry out direct determinations of the triplet scattering length for ^{87}Rb , relevant to Bose-Einstein condensation experiments, and of the $\text{Rb}+\text{Rb}$ C_6 dispersion coefficient. Consequences for the ^{85}Rb scattering length are discussed. [S1050-2947(97)07201-6]

PACS number(s): 34.50.Rk, 33.70.Ca, 32.80.Pj

I. INTRODUCTION

A fascinating aspect of the recent successful Bose-Einstein condensation (BEC) experiments in cold-gas samples of ^{87}Rb , ^7Li , and ^{23}Na atoms [1] is its close resemblance to the ideal gas BEC paradigm as it was originally predicted by Bose and Einstein [2]. In fact, instead of the complicated particle interactions involved in other laboratory BEC phenomena, the atom-atom interaction enters the description of the phase transition in an ultracold dilute gas only in the form of a single parameter, the scattering length a . On the time scale of the two-body collisions any atomic gas behaves like a hypothetical gas with the same value of a but without bound two-body states. The (in)stability of the Bose condensate is one of the properties that are fully determined by a . It is believed that in a homogeneous gas a Bose condensate is stable only for positive a [3,4]. In a trap it is possible to form a condensate with a long lifetime also for $a < 0$ if the total number of atoms is below a certain maximum [5,6], but in this case too a is a crucial quantity governing the equilibrium and nonequilibrium condensate properties.

The significance of the two-body collision parameters in atomic gases is not restricted to BEC experiments. For instance, the accuracy of recent improved versions of the cesium atomic frequency standard based on a fountain of laser-cooled atoms depends critically on elastic collisions among the atoms during their fountain orbit [7].

Several methods have been developed to obtain reliable information on such cold collision properties. The most direct method is a measurement of the elastic cross section in an experiment at sufficiently low temperature [8,9], which does not determine the sign of a , however. A second method is based on measuring the density-dependent frequency shift of a fountain clock [10]. A third method consists of extrapolation from the highest part of the bound-state spectrum through $E=0$, i.e., by inferring triplet- and singlet-scattering lengths a_T and a_S from (differences of) energies of the highest bound triplet and singlet states [11–13]. A fourth method that has recently proven to be very powerful is based on photoassociation spectroscopy [14–18], which can directly measure the oscillations of the continuum wave function for low positive E [14,18,19].

In this paper, we consider a combination of the latter two methods. Using photoassociation spectroscopy we observe a strong d -wave shape resonance in the scattering of two doubly spin-polarized ^{87}Rb atoms. From our data we derive the resonance energy, which restricts the ^{87}Rb triplet-scattering length as strongly as the energy of the last bound state would. This resonance energy provides a more restrictive determination of the scattering length than the Franck-Condon factors alone that we previously used [18], because the Franck-Condon factors determine the phase of the scattering wave function only in the radial range where the laser excitation occurs, and it is still necessary to extrapolate the wave function to infinite range using a van der Waals long-range interaction coefficient C_6 of limited accuracy. The energy of the quasibound resonance state, lying so close to threshold, is precisely the additional information needed to eliminate this degree of freedom from the analysis. In the following we will demonstrate this more explicitly (see Fig. 4 and accompanying discussion). This allows us to carry out direct determination of the $^{87}\text{Rb}+^{87}\text{Rb}$ triplet-scattering length, i.e., not via ^{85}Rb , and of the $\text{Rb}+\text{Rb}$ C_6 dispersion coefficient. While the previous determination [18] of $a_T(^{87}\text{Rb})$ rested on a theoretical C_6 value [20] and on mass-scaling a result for ^{85}Rb to ^{87}Rb using a theoretical number of bound triplet s -wave states, we are now able to dispense with these and still obtain a much narrower a_T range. The mass-scaling estimate uses the relation

$$v_D(^{87}\text{Rb}) = v_D(^{85}\text{Rb}) \sqrt{\frac{m(^{87}\text{Rb})}{m(^{85}\text{Rb})}}, \quad (1)$$

based on the WKB approximation, with v_D the (fractional) vibrational quantum number for $l=0$ at dissociation [21]. The analysis of a photoassociation experiment does not give information on the integer part of v_D , i.e., on the number of bound states $n_b - 1$. Together with the uncertainty in C_6 , this yielded a range $+85 < a_T(^{87}\text{Rb}) < +200a_0$ [18]. In the present paper we derive a much more restricted a_T value and also an improved value for the $\text{Rb } 5S-5P$ dipole matrix ele-

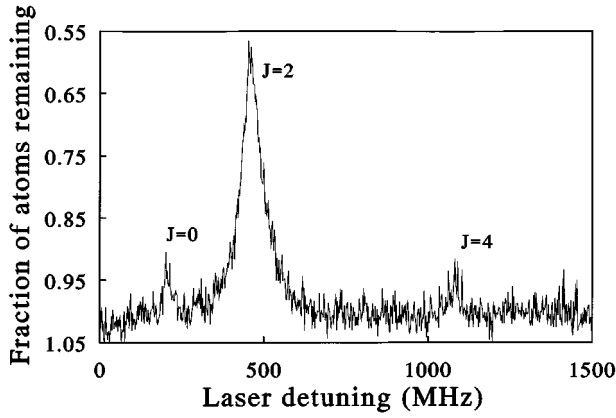


FIG. 1. Measured rotationally resolved photoassociation spectrum of a single 0_g^- vibrational level 5.9 cm^{-1} below the $5^2S_{1/2} + 5^2P_{1/2}$ limit, showing strong $J=2$ excitation.

ment, and obtain an indirect measurement of the number of $^{87}\text{Rb}_2$ triplet bound states.

II. EXPERIMENT AND ANALYSIS

The experiment is similar to that of Ref. [18]. About 10^4 ^{87}Rb atoms are loaded into a far-off-resonance optical-dipole force trap (FORT) [22], which has a wavelength of 808 nm, a waist of 11 micrometers, and a time-averaged potential well depth of 5 mK. These atoms are exposed to a combination of laser fields for 200 ms. This period is divided into repeated $5 \mu\text{s}$ cycles. During the first $2.5 \mu\text{s}$ of each cycle only the trapping (FORT) laser is on. During the next $0.6 \mu\text{s}$ of each cycle only two optical pumping laser beams are on, which maintain the atoms in their doubly spin-polarized $5^2S_{1/2}(F=2, M_F=2)$ sublevel. During the last $1.9 \mu\text{s}$ of each cycle, only the photoassociation (PA) laser beam is on, which is linearly polarized perpendicular to the quantization axis, and has an intensity in the range from 20 to 1000 W cm^{-2} .

At the end of each 200 ms period, we probe the atoms remaining in the trap with laser-induced fluorescence. If the PA laser is tuned to a photoassociation resonance, colliding pairs of atoms are optically excited to bound excited molecular states. These pairs decay back to the ground state by spontaneous emission. For the excited states we study, consideration of the Franck-Condon factors shows that virtually all of these spontaneous decays are to free pairs of atoms which are too energetic to remain in the trap, with the exception of a few percent that may decay to bound ground molecular states [23]. This loss of atoms from the trap results in a detectable change in the fluorescence level. We build up a spectrum by repeating the loading, 200 ms irradiation period, and fluorescence probe cycle for a succession of laser frequencies.

A typical photoassociation spectrum of a single vibrational level belonging to the 0_g^- state asymptotic to the $5^2S_{1/2} + 5^2P_{1/2}$ limit is shown in Fig. 1. A simple rotational spectrum is observed, with $J = 0, 2,$ and 4 lines visible. The most obvious feature of the data is the large size of the $J = 2$ peak, which is about 50 times larger than the $J=0$ peak when saturation effects are accounted for. As discussed be-

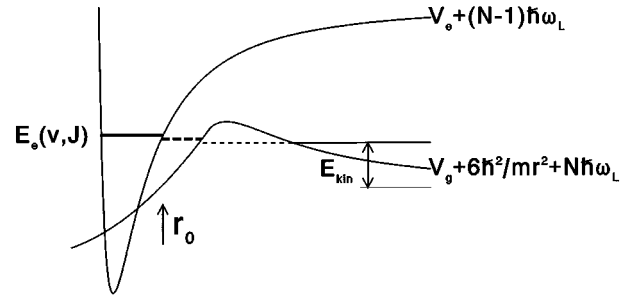


FIG. 2. Dressed-states picture of photoassociation process, including schematic ground-state and excited-state potentials. Changing the laser frequency ω_L , the excited bound-state energy shifts over the Maxwellian energy distribution in incoming channel, causing a peak in photoassociation spectrum. Shape resonance within $l=2$ centrifugal barrier enhances photoexcitation of $E_e, J=2$ state.

low, this large $J=2$ peak arises due to a d -wave shape resonance in the ground-state collision.

In a photoassociation collision two Rb ground-state atoms move along a potential V_g , absorb a photon from the PA laser and thereby undergo a transition to a bound $\text{Rb}+\text{Rb}^*$ state in an excited-state potential V_e . In a dressed-state picture schematically represented in Fig. 2 the bound state, which has already a width γ_0 for spontaneous emission, is embedded in the ground-state continuum and thus turns into a Feshbach resonance with an additional width γ_L for laser-induced continuum decay. Changing ω_L shifts the Maxwellian distribution in the ground-state channel over the resonance, thereby giving rise to a peak in the photoassociation spectrum.

The large $J=2$ peak may be easily understood from this picture. As has been discussed previously [18], for this spectrum the selection rule $J = l$ is obeyed, where l is the orbital angular momentum of the colliding atoms. The $l=2$ centrifugal barrier, at $140a_0$, is 0.42 mK high, as a summation of dispersion parts and centrifugal term shows. On the other hand, the optical excitation occurs at $r_0 \approx (40-48)a_0$ [18], the range of the outer turning points of the excited states involved. Both for the estimate of height and position of the barrier and for that of the range of outer turning points *ab initio* calculated potentials suffice [24–26]. Therefore, the $J=2$ peak measures the d -wave amplitude inside the centrifugal barrier. Its large size is due to the resonant buildup of this amplitude behind the barrier.

Information on the ground-state radial wave function $u_g(r)$ is contained in the peak heights and shapes, in particular in the partial width γ_L for decay of the shape resonance by laser excitation [18]:

$$\gamma_L = I_L \left| c \int u_e(r) d_{eg}(r) u_g(r) dr \right|^2, \quad (2)$$

with I_L the laser intensity, c a geometrical coefficient containing the full spin-angle structure, $u_e(r)$ the excited-state radial wave function, and $d_{eg}(r)$ the transition electric-dipole moment. γ_L occurs in the Breit-Wigner expression [27] for the squared S -matrix element for photoassociation:

$$|S_{PA}|^2 = \frac{\gamma_0 \gamma_L}{(\epsilon + E_g + \hbar \omega_L - E_e)^2 + \frac{1}{4} \gamma_0^2}, \quad (3)$$

in the notation of Ref. [18]. Both u_e and d_{eg} follow from the solution of a two-level problem in the 0_g^- subspace: A sum of 2×2 matrices for the asymptotic fine-structure splitting, a resonant electric dipole interaction V_{dip} , and a dispersion part is diagonalized in the separated-atom basis [25]. This determines both $V_e(r)$ and the structure of the 0_g^- electronic state. It turns out that the electric-dipole matrix-elements $d(P_{1/2})$ and $d(P_{3/2})$ of the atomic D lines entering V_{dip} are the most uncertain part of the analysis. A set of measured 0_g^- excited state level positions allows us to reduce this uncertainty sufficiently. We select a radius r_1 within but as close as possible to the outer turning point r_0 such that the local phase of the radial wave function is a linear function of energy over the small energy range involved. Calculations using an *ab initio* potential indicate that V_e is deep enough to choose $r_1 = 30a_0$ for $r_0 = (40-48)a_0$. This implies that the entire inner part of the potential can be described by two phase parameters only. We calculate bound-state energies assuming phase values at a fixed energy for ^{87}Rb and ^{85}Rb , as well as energy derivatives connected by mass scaling, and values for $d(P_{1/2})$ and $d(P_{3/2})$. Since the interatomic distances involved are close to the separated-atom limit, V_{dip} is a small perturbation compared to the fine-structure splitting. Furthermore, the $S_{1/2} + P_{1/2}$ expectation value of V_{dip} vanishes due to angular momentum selection rules, so that the first-order perturbation energy is zero. In second order only the nondiagonal matrix element comes in, i.e., the product $d(P_{1/2})d(P_{3/2})$. Due to the long distances the dependence of the analysis on the $n \geq 8$ ground-state and $n \geq 6$ excited-state dispersion coefficients is weak. We take them from Ref. [20] and [24] and include their uncertainty in the final error limits. Comparing theoretical levels with sets of $J=0$ levels for ^{85}Rb [18] and $J=2$ levels for ^{87}Rb (this experiment), we find optimal values for the three phase parameters and a value $d(P_{1/2})d(P_{3/2}) = 8.8 \pm 0.1$, thus improving the accuracy of our previous determination of this product [18].

Since $u_e(r)$ and $d_{eg}(r)$ can thus be derived from an analysis of frequencies of photoassociation peaks, γ_L is a ‘‘fingerprint’’ of the nodes of $u_g(r)$. At the large distances contributing to the integral (2) the required information on $u_g(r)$ can be summarized in a single unknown phase at r_1 , while a C_6 dispersion coefficient governs the development of $u_g(r)$ outside r_1 . Alternatively [18], one may take C_6 and v_D , the (fractional) vibrational quantum number for $l=0$ at dissociation [21]), or C_6 and a_T as equivalent pairs of parameters.

Figure 3 shows the measured relative $J=2$ peak areas (proportional to γ_L) for a number of 0_g^- vibrational states. A well-developed oscillation is visible of the kind one would expect from the simple Franck-Condon picture where the radial integral (2) is dominated by its contribution from near the outer turning point r_0 of $u_e(r)$ [14]. In Fig. 4(a) we present the strip in the v_D - C_6 plane, resulting from the re-

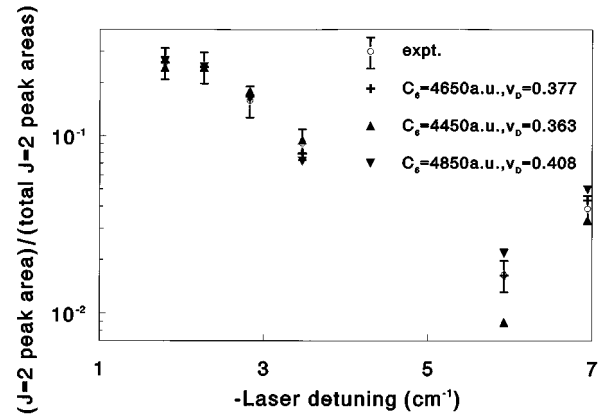


FIG. 3. ^{87}Rb $J=2$ peak areas measured for a number of 0_g^- vibrational states, showing Franck-Condon oscillation (circles), together with theoretical values for optimal χ^2 (plusses), together with theoretical values for two points on edges of χ^2 strip (triangles).

quirement that $u_g(r)$ has a node at the Franck-Condon radius corresponding to the node position in Fig. 3. We also indicate in Fig. 4(a) the strip where a shape resonance occurs below the top of the $l=2$ centrifugal barrier and that for the smaller energy range between 50% and 90% of the total barrier height following from the analysis below, taking the actual $J=2$ enhancement into account. This illustrates

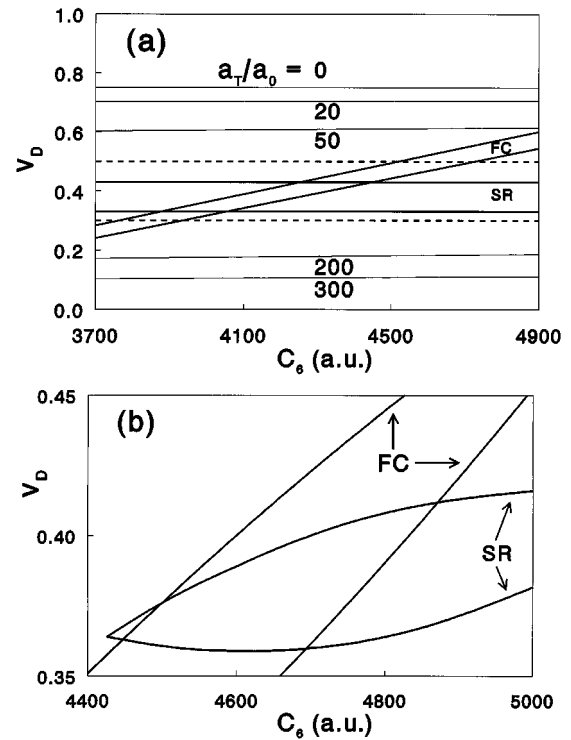


FIG. 4. Franck-Condon (FC) and shape-resonance (SR) strips in v_D - C_6 plane. (a) Strips following from simple picture. Dashed lines: strip for shape resonance below top of $l=2$ barrier. Thin lines: contour lines for a_T in units a_0 . (b) Strips following from ^{87}Rb analysis.

TABLE I. Scattering lengths in a_0 , determined from ^{85}Rb and ^{87}Rb analyses for $4400 < C_6 < 4900$ a.u.

Results from analysis of	$a_T(^{87}\text{Rb} + ^{87}\text{Rb})$		$a_T(^{85}\text{Rb} + ^{85}\text{Rb})$
^{87}Rb	$+99 < a_T < +119$	scaling →	$-\infty < a_T < -80$
^{85}Rb	$+85 < a_T < +200$	scaling ←	$-1200 < a_T < -10$

clearly the important role of the shape resonance in our analysis: in contrast to Ref. [18] we do not need a theoretical C_6 value as a second ingredient besides the Franck-Condon oscillations to determine the two unknown parameters.

The actual analysis starts with the determination of a temperature from the $J=2$ lineshapes for a grid of v_D and C_6 values. This temperature is used to calculate theoretical $J=0$ and $J=2$ peak areas. Two χ^2 functions then define the extent of agreement with experiment: a ‘‘shape-resonance-type’’ χ_1^2 corresponds to the ratio of the $J=2$ and $J=0$ peak areas for the peaks at detunings of 5.931 and 6.944 cm^{-1} , a ‘‘Franck-Condon-type’’ χ_2^2 is associated with the ratios of the areas of all ten measured $J=2$ peaks. The resulting strips in the v_D - C_6 plane, presented in Fig. 4(b), are in qualitative agreement with the schematic picture of Fig. 4(a). Clearly, the more rigorous analysis on the basis of the radial integral (2) effectively shifts the outer nodes in $u_g(r)$ over a small distance inward, which tends to decrease the local wavelength and increase C_6 . We find the two criteria to set independent strips in the parameter plane with an intersection leading to $0.35 < v_D < 0.42$ and $4400 < C_6 < 4900$ a.u. The temperature turns out to be 0.25 ± 0.05 mK. This temperature is consistent with our previous studies of the FORT [22] in which we determined that our loading method typically produces clouds of atoms with a temperature in the range of 0.15–0.50 mK. The values for v_D and C_6 together determine the scattering length. We find the limits $+99a_0 < a_T < +119a_0$, narrower than the range $+85a_0 < a_T < +140a_0$ in Ref. [18], and obtained with less input of information from theory.

III. DISCUSSION AND CONCLUSION

Let us now discuss the consequences for the ^{85}Rb scattering length. If we use mass scaling, assigning an upper limit ± 3 for the error bar on the number 38 of s -wave triplet bound $^{87}\text{Rb}_2$ states (n_b) derived from the Krauss-Stevens *ab initio* triplet potential [26], we find a_T to be negative (see Table I) for the entire above C_6 range. This is consistent with an analysis based on direct ^{85}Rb measurements and the same C_6 -range (Table I), extending the ^{85}Rb data analyzed in Ref. [18] with an additional set of data obtained more recently, also leading to negative a_T values only. The new direct ^{85}Rb results are also consistent with Ref. [18], leading, however, to a narrower range of v_D values: $-0.23 < v_D < -0.03$.

There are no experimental results on a_T from other experimental methods available in the literature. We note that

the measurement of the elastic cross section by Newbury, Myatt, and Wieman [8] was carried out for the nonstretched $|1, -1\rangle$ spin state in which both triplet and singlet contributions are involved. We are presently extending our work to include the mixed triplet-singlet channels. The measured value of $|a_{1,-1}|$ is one of the experimental data that have to be taken into account in this work. Note that the scattering length for the spin-stretched state $|2, +2\rangle$ does not depend on the magnetic field, in contrast to that for the B -dependent $|1, -1\rangle$ state. As a consequence, Feshbach resonances at specific field values, where the scattering length changes sign, are not expected.

Our measured C_6 value is consistent with a recent theoretical value of 4426 a.u. [20]. This calculation should have an accuracy which is comparable to or better than our measurement, since it is derived from a model which reproduces accurately known atomic properties of Rb including its polarizability. Allowing for a maximum deviation of C_6 from 4426 a.u. by 4% restricts $a_T(^{85}\text{Rb})$ to the least negative values and hardly changes $a_T(^{87}\text{Rb})$.

Finally, we can directly compare the ^{85}Rb and ^{87}Rb photoassociation spectra. Intensities of $J=0$ lines in the ^{85}Rb spectrum are generally much larger than for ^{87}Rb with comparable PA laser intensity. This behavior may be understood from the limiting form of the scattering wave function at low energy [19]. For all parameters in Table I ratios between theoretical ^{85}Rb and ^{87}Rb peak areas are consistent with experimental ratios.

We may also use the condition that mass scaled results of the separate ^{85}Rb and ^{87}Rb analyses are consistent to derive the number of bound states in the $^{87}\text{Rb}_2$ triplet ground state. We determine $n_b = 42 \pm 4$, in good agreement with the theoretical value 38 derived from Ref. [26]. To our knowledge, there is no experimental information on this quantity.

From these parameter values the tunneling lifetime γ_t^{-1} of the $l=2$ shape resonance is calculated to be in the range 20–100 ns, not very different from the spontaneous emission lifetime γ_0^{-1} and from the time scale of the photoassociation process γ_L^{-1} for easily attainable laser intensities. It should therefore be possible to obtain direct information on the time it takes the atoms to tunnel through the barrier and form the shape resonance by suitable time-dependent photoassociation measurements.

In conclusion, we have observed a shape resonance in the collision of two cold ^{87}Rb atoms. Its existence has made it possible to carry out direct determination of the ^{87}Rb triplet-scattering length without relying on a mass-scaling argument and a theoretical C_6 value. Nevertheless we find a much narrower positive interval. Likewise, we have obtained a more reliable and negative a_T range for ^{85}Rb . This information is relevant for present BEC experiments in rubidium gas samples. Finally, we have extracted a ground-state C_6 value with a 5% error limit and the number of bound states supported by the ^{87}Rb triplet potential with a 10% error limit.

ACKNOWLEDGMENTS

We gratefully acknowledge the support of work at Austin by the A. P. Welch Foundation and the National Science Foundation, and work at Eindhoven by the Nederlandse Organisatie voor Wetenschappelijk Onderzoek NWO.

- [1] M.H. Anderson, J.R. Ensher, M.R. Matthews, C.E. Wieman, and E.A. Cornell, *Science* **269**, 198 (1995); C.C. Bradley, C.A. Sackett, J.J. Tollet, and R.G. Hulet, *Phys. Rev. Lett.* **75**, 1687 (1995); K.B. Davis, M.-O. Mewes, M.R. Anderson, N.J. van Druten, D.S. Durfee, D.M. Kurn, and W. Ketterle, *ibid.* **75**, 3969 (1995).
- [2] S.N. Bose, *Z. Phys.* **26**, 178 (1924); A. Einstein, *Sitzungsber. Kgl. Preuss. Akad. Wiss.* **1924**, 261 (1924).
- [3] A.L. Fetter and J.D. Walecka, *Quantum Theory of Many-Particle Systems* (McGraw-Hill, New York, 1971), p. 218.
- [4] E. Tiesinga, A.J. Moerdijk, B.J. Verhaar, and H.T.C. Stoof, *Phys. Rev. A* **46**, R1167 (1992).
- [5] P.A. Ruprecht, M.J. Holland, K. Burnett, and M. Edwards, *Phys. Rev. A* **51**, 4704 (1995).
- [6] Yu. Kagan, G.V. Shlyapnikov, and J.T.M. Walraven, *Phys. Rev. Lett.* **76**, 2670 (1996).
- [7] K. Gibble and S. Chu, *Metrologia* **29**, 201 (1992).
- [8] N.R. Newbury, C.J. Myatt, and C.E. Wieman, *Phys. Rev. A* **51**, R2680 (1995).
- [9] K.B. Davis, M.-O. Mewes, M.A. Joffe, M.R. Andrews, and W. Ketterle, *Phys. Rev. Lett.* **74**, 5202 (1995).
- [10] B.J. Verhaar, K. Gibble, and S. Chu, *Phys. Rev. A* **48**, R3429 (1993).
- [11] A.J. Moerdijk, W.C. Stwalley, R.G. Hulet, and B.J. Verhaar, *Phys. Rev. Lett.* **72**, 40 (1994).
- [12] A.J. Moerdijk and B.J. Verhaar, *Phys. Rev. Lett.* **73**, 518 (1994).
- [13] E.R.I. Abraham, W.I. McAlexander, C.A. Sackett, and R.G. Hulet, *Phys. Rev. Lett.* **34**, 1315 (1995).
- [14] J.D. Miller, R.A. Cline, and D.J. Heinzen, *Phys. Rev. Lett.* **71**, 2204 (1994); R.A. Cline, J.D. Miller, and D.J. Heinzen, *ibid.* **73**, 632 (1994).
- [15] L.P. Ratliff, M.E. Wagshull, P.D. Lett, S.L. Rolston, and W.D. Phillips, *J. Chem. Phys.* **101**, 2638 (1994).
- [16] W.I. McAlexander, E.R.I. Abraham, N.W.M. Ritchie, C.J. Williams, H.T.C. Stoof, and R.G. Hulet, *Phys. Rev. A* **51**, 871 (1995).
- [17] R. Napolitano, J. Weiner, C. J. Williams, and P. S. Julienne, *Phys. Rev. Lett.* **73**, 1352 (1994).
- [18] J.R. Gardner, R.A. Cline, J.D. Miller, D.J. Heinzen, H.M.J.M. Boesten, and B.J. Verhaar, *Phys. Rev. Lett.* **74**, 3764 (1995).
- [19] R. C. Côté, A. Dalgarno, Y. Sun, and R. G. Hulet, *Phys. Rev. Lett.* **74**, 3581 (1995).
- [20] M. Marinescu, H.R. Sadeghpour, and A. Dalgarno, *Phys. Rev. A* **49**, 982 (1994).
- [21] The actual analysis makes use of a more rigorous scaling relation: that between the phases ϕ of the oscillating radial wave functions [18].
- [22] J.D. Miller, R.A. Cline, and D.J. Heinzen, *Phys. Rev. A* **47**, R4567 (1993).
- [23] H.R. Thorsheim, J. Weiner, and P.S. Julienne, *Phys. Rev. Lett.* **58**, 2420 (1987).
- [24] M. Marinescu and A. Dalgarno, *Phys. Rev. A* **52**, 311 (1995).
- [25] M. Movre and G. Pichler, *J. Phys. B* **10**, 2631 (1977).
- [26] M. Krauss and W.J. Stevens, *J. Chem. Phys.* **93**, 4236 (1993).
- [27] H. Feshbach, *Theoretical Nuclear Physics, Part 1: Nuclear Reactions* (Wiley, New York, 1992).